

Simulation and visualization of the displacement between CO₂ and formation fluids at pore-scale levels and its application to the recovery of shale gas

Peng Hou¹ · Yang Ju^{1,3} · Feng Gao^{1,2} · Jianguo Wang² · Jian He¹

Received: 1 October 2016 / Revised: 17 November 2016 / Accepted: 1 December 2016 / Published online: 4 January 2017
© The Author(s) 2017. This article is published with open access at Springerlink.com

Abstract This article reports recent developments and advances in the simulation of the CO₂-formation fluid displacement behaviour at the pore scale of subsurface porous media. Roughly, there are three effective visualization approaches to detect and observe the CO₂-formation fluid displacement mechanism at the micro-scale, namely, magnetic resonance imaging, X-ray computed tomography and fabricated micromodels, but they are not capable of investigating the displacement process at the nano-scale. Though a lab-on-chip approach for the direct visualization of the fluid flow behaviour in nanoscale channels has been developed using an advanced epi-fluorescence microscopy method combined with a nanofluidic chip, it is still a qualitative analysis method. The lattice Boltzmann method (LBM) can simulate the CO₂ displacement processes in a two-dimensional or three-dimensional (3D) pore structure, but until now, the CO₂ displacement mechanisms had not been thoroughly investigated and the 3D pore structure of real rock had not been directly taken into account in the simulation of the CO₂ displacement process. The status of research on the applications of CO₂ displacement to enhance shale gas recovery is also analyzed in this paper. The coupling of molecular dynamics and LBM in tandem is proposed to simulate the CO₂-shale gas displacement process based on the 3D digital model of shale obtained from focused ion beams and scanning electron microscopy.

Keywords CO₂-formation fluid displacement · Micro- and nano-pore scale · Shale gas recovery · Lattice Boltzmann methods · Molecular dynamics · FIB-SEM

1 Introduction

CO₂, as one of the greenhouse gases, plays a key role in the cause of global warming, and its accumulation in the atmosphere is still increasing (Allen et al. 2014). As a

result, CO₂ mitigation has attracted increasing attention (Edenhofer et al. 2014). CO₂ capture and sequestration (CCS) technology is an alternative to effectively reduce the CO₂ emission in the short term (IEA 2013). Popularly, brine or saline aquifers, oceans, depleted oil reservoirs, and coal beds are considered potential geological formations for CO₂ storage. For example, Fujii et al. (2010) and Zahid et al. (2011) argue that saline aquifers are the most viable alternative to store CO₂ because they possess the greatest potential for carbon storage and wide geographical spread. Other studies suggest that CO₂ is a working fluid that can be used to enhance oil recovery (EOR) and natural gas recovery (EGR) (Hughes et al. 2012; Liu et al. 2015a, b; Middleton et al. 2015). Injecting CO₂ into oil or gas reservoirs is promising because it can also offset the costs of CCS (Koide et al. 1992; Blunt et al. 1993; Gunter et al. 1997). When CO₂ is injected into a deep geological

✉ Yang Ju
juy@cumtb.edu.cn; yju@icould.com

¹ State Key Laboratory for Geomechanics & Deep Underground Engineering, China University of Mining & Technology, Xuzhou 221116, China

² School of Mechanics & Civil Engineering, China University of Mining & Technology, Xuzhou 221116, China

³ State Key Laboratory of Coal Resources & Safe Mining, China University of Mining & Technology at Beijing, Beijing 100083, China

formation in the liquid or supercritical state, it will cause large volumes of formation fluids such as oil, water (brine) or natural gas to be physically displaced (Kazemifar et al. 2016; Wang et al. 2013; Zhang et al. 2011b). In the CO₂ displacement process, the major concern is the primary CO₂ plume migration, which is closely related to how much CO₂ can be stored in the respective porous subsurface sedimentary formation, the displacement efficiency of the oil/gas and the security of the stored CO₂ (Berg and Ott 2012; Chen and Zhang 2010; Song et al. 2014). Therefore, a better understanding of the displacement mechanisms of CO₂ and formation fluids in porous media is essential to assess the CO₂ leakage risks and predict the amount of CO₂ that can be absorbed and the oil/gas production as well.

Predicting changes in the flow and transport properties of CO₂ and formation fluids in porous rock is still a challenging issue owing to the multi-phase flow, complexity of the fluid–rock interactions and intrinsic heterogeneity of porous rocks (Garcia-Rios et al. 2015). Thus, the CO₂ displacement process in porous media has attracted increasing attention. Extensive research on CO₂ displacement has been performed over multiple spatial scales that range from a few nanometres to tens or hundreds of kilometres, and it is also clear that the appropriate methods to be employed vary between different scales. At the macro-scale, average properties must be employed, as an explicit description of the pore-scale phenomena is simply impossible. Additionally, the physical and chemical processes occur in discontinuous pore geometries and are controlled by interfacial processes, which have a large influence on the large-scale phenomena of the system and ultimately require a pore-scale perspective for obtaining a better understanding of the mechanisms (Blunt et al. 2013; Wildenschild and Sheppard 2013; Ferrari 2014; Morais et al. 2016). In the last decades, the pore-scale modelling of CO₂-formation fluid displacement has been promoted by three factors: the recent advances in porous media characterizations by visualization techniques, some novel numerical theories, and advances in high-performance computing (Ferrari 2014). However, studies on the CO₂-formation fluid displacement using these promising technical and theoretical approaches have not been systematically analysed in the published literature.

Thus, the objective of this contribution is to outline the recent developments and advances in the simulation and visualization of the CO₂-formation fluid displacement process occurring at the micro-scale and nano-scale—also referred to here as the pore-scale—and to highlight perspectives for future research. In Sect. 2, some relevant important processes and characterizations of the CO₂-formation fluid displacement are briefly discussed. In Sect. 3, several novel visualization techniques and numerical simulation methods for the CO₂-formation fluid displacement are introduced in detail, including a discussion of their strengths and weaknesses. Finally, Sect. 4 provides a

comprehensive overview of the applications of CO₂ displacement to enhanced shale gas production including the status of research, challenges and possible solutions.

2 Characterizations of the CO₂-formation fluid displacement

2.1 Viscous fingering

In porous media, viscous and capillary forces play key roles in impacting the CO₂-formation fluid displacement. The injected CO₂ viscosity is generally lower than that of formation fluids (Nordbotten et al. 2005), and the interfacial tension between the CO₂ and formation fluids depends on the pressure, temperature, and other system conditions (Chiquet et al. 2007; Espinoza and Santamarina 2010). Two dimensionless parameters, namely, the capillary number (Ca) and viscosity ratio (M), are commonly employed to describe the various forces encountered by the two fluids during their displacement in the porous media. These two parameters are defined as

$$Ca = \frac{\mu_2 V_2}{\gamma \cos \theta} \quad (1)$$

$$M = \frac{\mu_2}{\mu_1} \quad (2)$$

where μ_1 and μ_2 are the viscosity of the displacing fluid and the viscosity of the displaced fluid, respectively. V_2 is the bulk velocity of the displacing fluid, γ is the interfacial tension between the two fluids, and θ is the fluid–fluid contact angle with the solid surface.

Based on the values of Ca and M , three displacement patterns can be identified, as shown in Fig. 1: viscous fingering, capillary fingering and stable displacement (Lenormand et al. 1988; Zhang et al. 2011a; Yamabe et al. 2015). In the CO₂ displacement process, the fluid flow speed is low in subsurface rocks ($Ca \ll 1$), and the viscosity ratio is considered to be less than 1 ($M < 1$) (Yamabe et al. 2015). Hence viscous fingering can commonly occur during the CO₂-formation fluid displacement. Viscous fingering is the formation of special fingers with morphologically unstable interfaces of the invading fluid. A deep understanding of viscous fingering is essential for accurately predicting the migration and transport of the injected CO₂ and formation fluids within the pore structure of the formations.

2.2 CO₂-rock interaction

With a deep understanding of the CO₂-formation fluid displacement process, the CO₂-rock interactions intervene

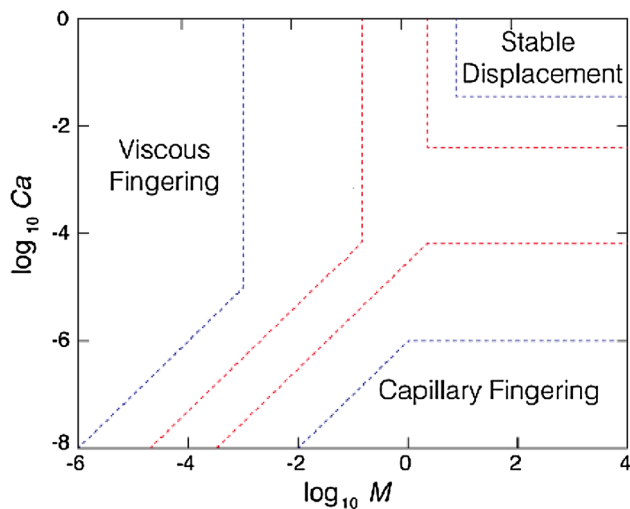


Fig. 1 Classification of displacement patterns based on Ca and M . The boundaries marked with *blue lines* are those noted by Lenormand et al. (1988), whereas those marked with *red lines* are those from Zhang et al. (2011a). Modified after Yamabe et al. (2015)

in more areas than initially anticipated, whereby certain areas have attracted less attention to date. When CO₂ is injected into formations, scCO₂ will dissolve, and interaction will occur between the CO₂ and formation rock (Gaus 2010). As a consequence, these interactions will lead to changes in the pore structure of the formation rock, decreasing the porosity and permeability of the rock. These changes in the pore geometry of the formation rock will seriously impact the fluid transport in the CO₂-formation fluid displacement. Thus, there are three key issues summarized in the review of Gaus (2010), that is, where do CO₂-rock interactions occur, what are the drivers of CO₂-rock interactions and what is their influence on the porosity and permeability, and how can the CO₂-rock interactions be assessed.

3 Displacement simulation and visualization

3.1 Experimental visualization

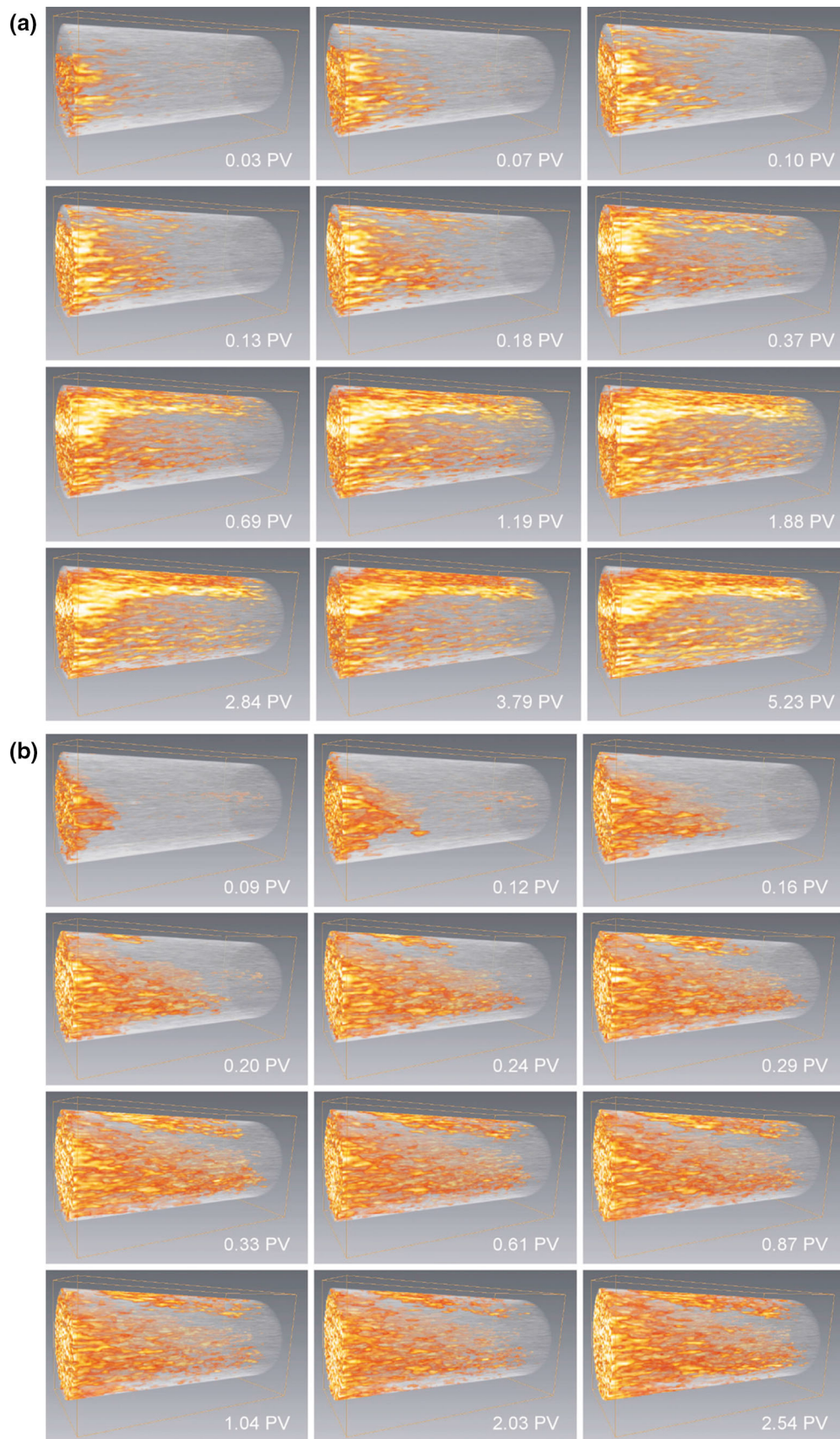
Laboratory experiments on CO₂-formation fluid displacement can provide valuable insights into processes that control the displacement process at the pore scale of porous media and improve our understanding of multi-phase flow. Pore-scale experiments also permit the evaluation of the constitutive relationships that are used in large-scale simulators (Dehoff et al. 2012). Roughly, there are three main visualization approaches to detect and observe CO₂ displacement processes at the pore scale: magnetic resonance imaging (MRI), X-ray computed tomography (CT) (Shi et al. 2009, 2011a, b; Zhao et al. 2011a; Alemu et al. 2013; Berg et al. 2013b) and fabricated micromodels (Ferer et al.

2004; Cottin et al. 2010; Zhang et al. 2011a; Wang et al. 2013; Al-Housseiny et al. 2012). These methods are recognized as effective approaches to directly characterize the transport properties of the displaced fluid and displacing fluid at the pore scale.

3.1.1 X-ray CT

X-ray CT is a non-invasive and non-destructive imaging technique used to characterize the internal physical structure of the sample and allow for the three-dimensional (3D) in situ visualization of the fluid phases (Lindquist et al. 1996; Hunt and Bajsarowicz 1988; Wellington and Vinegar 1985, 1987; Schlüter et al. 2014). The theories and devices of X-ray CT are described by Wildenschild and Sheppard (2013) in details. In the last decades, X-ray CT has been widely used to investigate CO₂-formation fluid displacement. For instance, Berg et al. (2010) investigated the miscible displacement performance of a CS₂-nC₁₀ system at 1.5 MPa and 25 °C using CT scanning. The authors concluded that the front fingering could affect the mixing zone area. Berg et al. (2013a) also studied the displacement and mass transfer between saturated and unsaturated CO₂-brine systems in sandstone using CT, and 3D saturation patterns during the injection were obtained (Fig. 2). Seo (2004) and Seo and Mamora (2005) conducted the first experimental study of enhanced gas recovery by injecting CO₂ through a dry carbonate core that was saturated with CH₄ at 20–80 °C and 3.55–20.79 MPa. The distribution of CH₄ and CO₂ in the core was obtained using an X-ray CT scanner at the breakthrough time. The recovery of CH₄ was 73%–87%, and the dispersion coefficient of CO₂ was approximately 0.0–0.12 cm²/min. In addition to the above studies using real reservoir rock cores, some researchers chose sand packs as an experimental material for basic research on the displacement process. Liu et al. (2015b) investigated the CO₂-CH₄ displacement process in sand packs, and the displacement process was scanned with a resolution of approximately 34.2 μm by an X-ray CT scanner. Concurrently, the dispersion coefficients were obtained, and the effects of the temperature, pressure, CO₂ injection flow rate and mean diameter of the glass beads were analysed. Through the X-ray CT scan, the detailed displacement process in the sand pack sample was obtained noninvasively, as shown in Fig. 3. The existence of the mixing zone was proven, and no interface appeared in the process of CO₂-CH₄ displacement.

However, based on previous studies, the front fingering and the mixing zone of the displacement process can only be qualitatively analysed by the CT imaging and cannot be quantified. Moreover, the microscopic fluid state cannot be detected using medical CT scanners owing to the insufficiently high resolution (millimetre-scale) compared with



◀ **Fig. 2** 3D saturation patterns (CO₂ in *red/yellow*), **a** unsaturated CO₂-brine systems and **b** saturated CO₂-brine systems. The rock matrix is visible as a semi-transparent background. The displacement shows the gravity over-run of CO₂. (Berg et al. 2013a)

the pore sizes, which could make the results of the experiments less credible. The resolution of nano-CT (50 nm) is high, but it takes a long time to collect one image unless fast synchrotron-based sources are used.

3.1.2 MRI

MRI is similar to X-ray CT in that non-invasive visualizations of the fluid movement and distribution can be

obtained in the core. The differences are that unprecedented quantitative information about the distribution of fluid sand information about the rock structure corresponding to local regions within the porous media can be provided by MRI during the displacement processes (Song et al. 2012). Special features of MRI include its abilities to measure the fluid flow velocities and to distinguish between different liquids by the differences in their intrinsic MRI properties, which are difficult to obtain by other methods. It also has a shorter measurement time and is much less hazardous in comparison with X-ray CT (Xiong et al. 2016). Using the MRI technique, some studies were performed on the CO₂-formation fluid displacement in porous media. Suekane et al. (2005, 2006, 2009) used

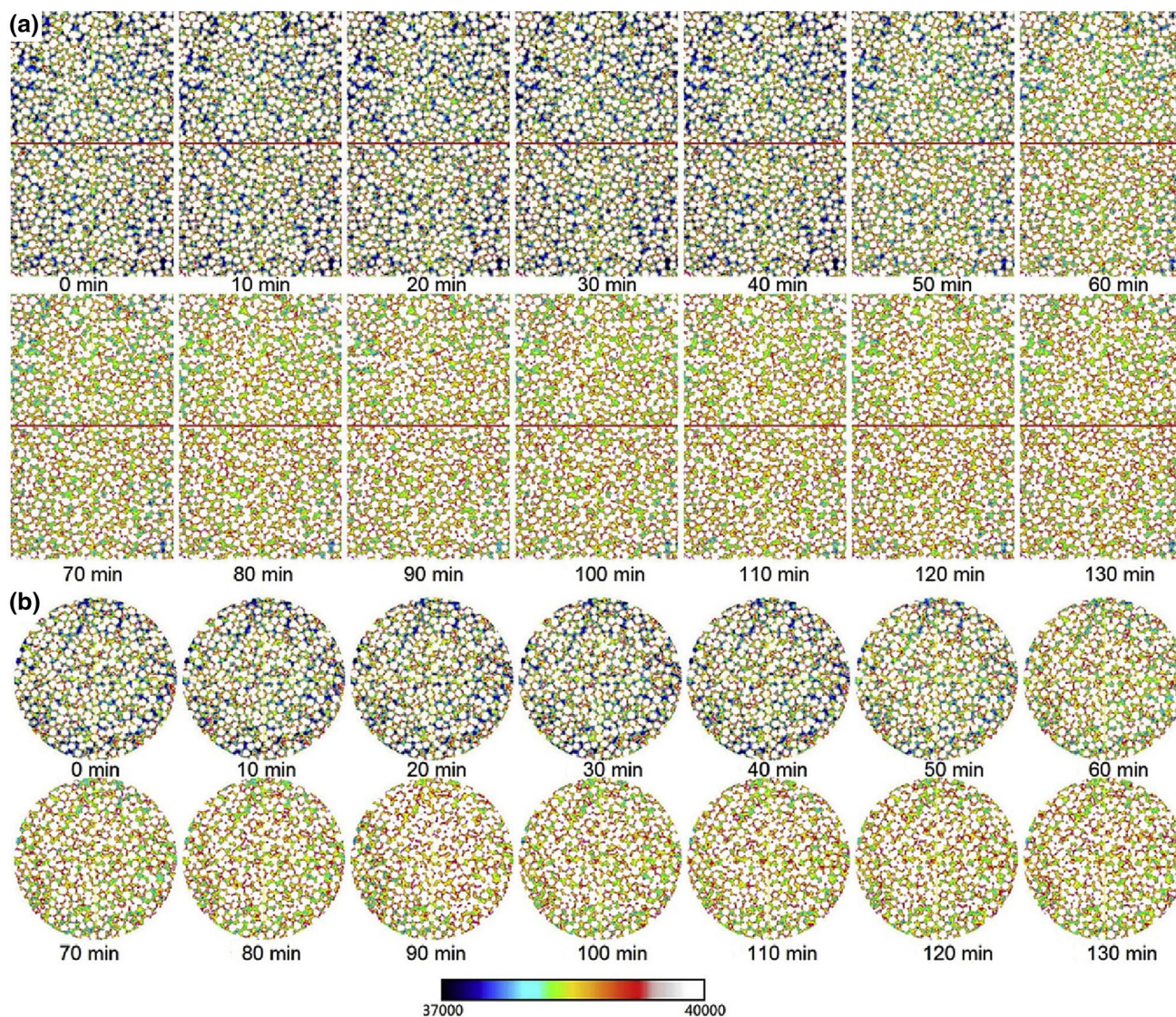


Fig. 3 **a** CT scan images of the same vertical section in displacement in the BZ04 glass bead sand pack sample with time; **b** corresponding CT scan images of the same middle cross-section located on the red line of the vertical section of (a); The colour scale is set based on grey scale, with glass beads painted as white with edges that may be red or yellow, blue and dark blue are CH₄, green represents CO₂, and cyan indicates a mixture of CH₄ and CO₂. (For the interpretation of the references to colour in this figure legend, the reader is referred to the web version of this article.) (Liu et al. 2015b)

the MRI technique to directly visualize the distribution of supercritical CO₂ (scCO₂) in a bead-pack core containing water at a certain temperature and pressure that approximate aquifers at a depth of approximately 1000 m. Liu et al. (2011) analysed the immiscible and miscible CO₂ displacement of oil in glass bead packs using MRI technology. In their study, the local Darcy velocities of CO₂ were acquired based on the oil saturation data obtained from MRI images, and the effects of the capillary pressure, viscosity and buoyancy on the CO₂ displacement process can also be evaluated using a special core flood analysis. Zhao et al. (2011a, b) proposed a method to calculate the average velocity of the CO₂ front and implemented CO₂–oil miscible displacement in a sand pack using MRI. The local Darcy phase velocities of the CO₂ and oil were calculated with this method and are shown in Fig. 4. Song et al. (2012) studied the CO₂–water displacement process in packed glass beads using high-resolution MRI. MRI images of the CO₂ displacement were obtained, and the effects of the displacement type, CO₂ injection flow rate and effective porosity were considered. A summary of the results of the displacement experiments is shown in Table 1. Song et al. (2014) also analysed the in situ mixing zone performance of CO₂–oil miscible displacement flows in a sand pack using MRI. The mixing zone length, CO₂ frontal velocities, longitudinal dispersion coefficient and Peclet number were quantified based on magnetic resonance imaging. Yang et al. (2015) investigated the dynamic stability characteristics of fluid flow in CO₂–oil miscible displacement using an MRI apparatus, and the CO₂ frontal velocities and mixing zone length were visually quantified.

Although a number of studies have been conducted to investigate the CO₂–formation fluid displacement in a sand pack using MRI, and some CO₂–formation fluid displacement mechanisms have been clearly analyzed, there have been almost no studies on natural rocks owing to the harsh conditions of MRI against the experimental materials. As the geometry of the natural rock sample is more complex than that of the sand packs, the reliability achieved for the previous experimental results can be compromised.

3.1.3 Fabricated micromodels

The rock cores have an advantage in characterizing individual formations, but on the pore scale, the fluid flow is difficult to monitor since sophisticated and unique microtomographic facilities are needed to visualize the internal distribution of the fluids within the rock cores. The natural media also presents other challenges in that the porosity, pore size, connectivity, and wetting properties are unable to be independently manipulated. These limitations can be

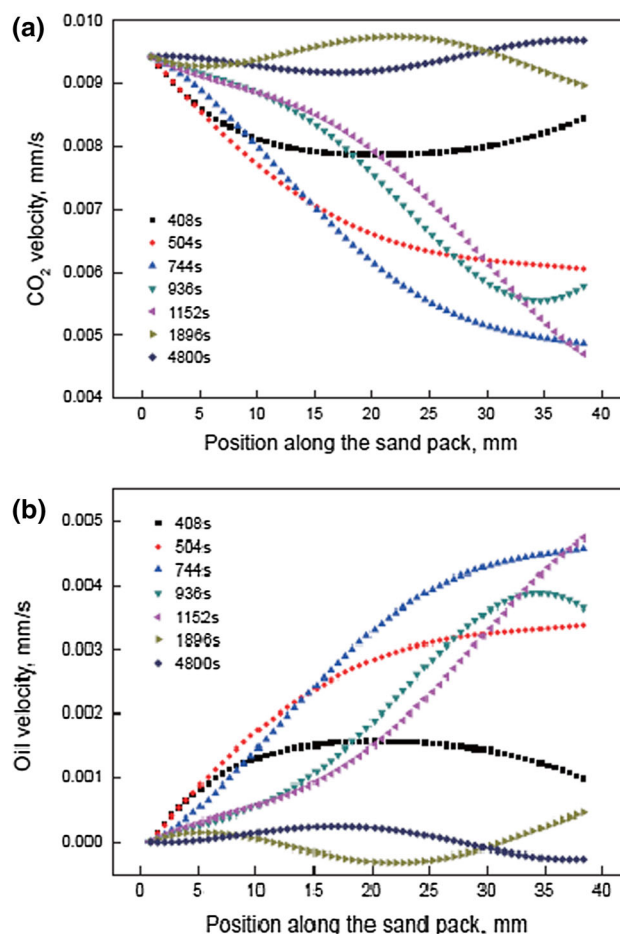
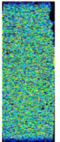
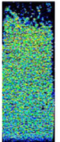
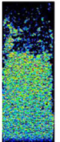
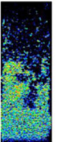
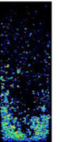
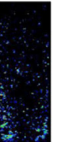

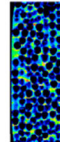
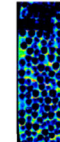
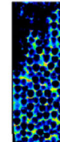
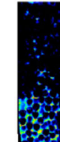
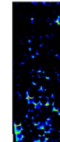
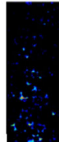
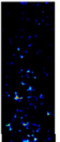
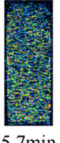
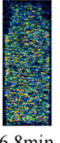
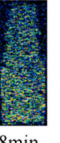
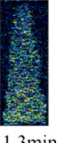
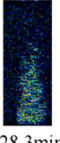
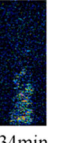

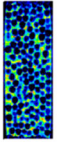
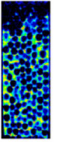
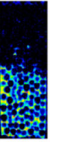
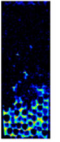
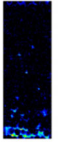
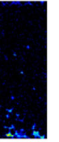
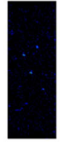
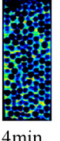
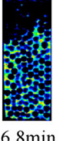
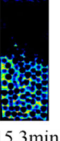
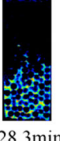
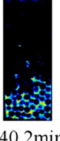
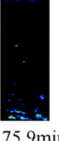
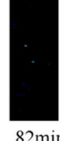


Fig. 4 Local phase velocities of a CO₂ and b oil. (Zhao et al. 2011b)

overcome by micromodels, which allow for the visualization of the fluid distribution using cameras with or without fluorescence microscopy. The subsequent quantification of the fluid transport and interfacial area may provide mechanistic insight into the physical fluid displacement process at the microscopic level. Experimental studies on the CO₂–formation fluid displacement have been widely conducted in 2D micromodels to reveal the mechanisms of the fluid displacement.

Er et al. (2010) investigated the porous matrix and fracture interaction during CO₂ injection into a glass micromodel initially saturated with oil, demonstrating the importance of the CO₂–oil interaction near the matrix–fracture interface. Chalbaud et al. (2009) visualized the scCO₂ displacement of water in glass micromodels, but the saturations of the fluids could not be quantified owing to difficulties in distinguishing between the fluids. Riazi et al. (2011) simulated CO₂–oil and CO₂–water displacement processes in an etched glass micromodel, and the results showed a faster CO₂ breakthrough in the micromodel saturated with oil than that with water. The above studies were all limited to qualitative visualizations of the fluid

Table 1 Summary of results for CO₂/water displacement experiments of Song et al. (2012)

| Displacement type | Effective porosity (%) | Flow rate (mL/min) | Visual displacement process | | | | | | | Displacement efficiency (%) |
|-------------------|------------------------|--------------------|--|--|--|--|---|--|--|-----------------------------|
| Immiscible | 40.0 | 0.03 |  |  |  |  |  |  |  | 70.9 |
| | | | 13min | 16.5min | 18min | 20.4min | 25.5min | 28.3min | 37.9min | |
| Immiscible | 37.32 | 0.03 |  |  |  |  |  |  |  | 77.7 |
| | | | 5.7min | 8.5min | 10.2min | 13min | 15.3min | 18min | 26.6min | |
| Miscible | 40.0 | 0.03 |  |  |  |  |  |  |  | 81.50 |
| | | | 5.7min | 6.8min | 8min | 11.3min | 28.3min | 34min | 79.3min | |
| Miscible | 37.32 | 0.03 |  |  |  |  |  |  |  | 83.5 |
| | | | 2.8min | 5.7min | 9.6min | 13min | 17min | 22.7min | 64.6min | |
| Miscible | 37.32 | 0.01 |  |  |  |  |  |  |  | 83.0 |
| | | | 4min | 6.8min | 15.3min | 28.3min | 40.2min | 75.9min | 82min | |

flow during the displacement process, and quantitative information about the interfacial areas and fluid saturations was not acquired. The study of Zhang et al. (2011b) was the first to quantitatively evaluate the influence of the capillary forces and porous media heterogeneity on the liquid CO₂-water displacement in a dual-permeability pore network micromodel using fluorescence microscopy. Wang et al. (2013) simulated the effects of the injection rates and injection methods on the scCO₂ displacement of water in a homogeneous micromodel, and the results of the simulation are quantitatively compared using the obtained fluorescent images. Kazemifar et al. (2016) quantified the flow dynamics of the scCO₂ displacement of water in a 2D porous micromodel by combining fluorescence microscopy and microscopic particle image velocimetry (PIV).

Unfortunately, micromodels lack the complex geometry of real media, which often have multiscale and random characteristics that will dictate the fluid and solute transport. In addition, these experimental studies used simple two-dimensional porous media. To overcome the above

limitations, Ju et al. (2014a) incorporated several advanced technologies, such as CT scan, three-dimensional (3D) reconstruction (Gomi et al. 2007; Geiger et al. 2009; Hajizadeh et al. 2011; Zhang et al. 2013; Birk et al. 2014; Ju et al. 2014b), and 3D printing, to produce a physical model representing the natural rock. A 3D digital image can be obtained to represent the real rock structure based on the high-resolution X-ray CT imaging and the reconstruction, and then its three-dimensional micromodel using transparent material can be generated using a 3D printer. This novel idea offers a very good opportunity to accurately investigate the properties of complex flows.

These experimental simulation methods greatly promote our understanding of the CO₂-formation fluid displacement mechanism. However, it is worth noting that these simulation experiments are performed based on the pore geometric characteristics of a conventional formation that has a minimum pore size on the micrometre scale. The pore sizes and pore throat radii of unconventional gas reservoirs range from 1 to 300 nm, which are much smaller than those of

conventional reservoirs with pore sizes in the range of 1–100 μm (Cipolla et al. 2009). These popular experimental simulation methods are thus not able to investigate fluid flow at the nano-metre scale because the maximum precision of these techniques is on the micro-metre scale in general. Special characteristic features that can be produced at the nanometre scale include a high capillary pressure, low porosity, and high wetting phase residue saturation (Wu 2014). Other transportation mechanisms may also occur. The displacements of two-phase flow in nano-pores are poorly understood. Wu (2014) developed a lab-on-chip approach for the direct visualization of the fluid flow behaviour in nanoscale channels using an advanced epi-fluorescence microscopy method combined with a nanofluidic chip. This method is expected to improve the understanding of the CO_2 displacement behaviour on the nano-scale. However, it is still a qualitative analysis method and cannot quantifiably reflect the displacement process.

3.2 Numerical simulation

A large number of the porous media studies on fluid displacement have been numerically performed, and numerical simulations can provide an economical and efficient pathway to explore the influences of the flow and physical parameters in various complicated porous media. Pore-scale simulations provide a level of information on flow characteristics that cannot be obtained in laboratory experiments, for example, the full pressure and velocity fields and the position of the interface. Modelling approaches of multiphase flow at the pore scale can be divided into two categories: direct simulations, in which the flow equations are directly solved on a discretized pore space obtained from images of rock cores, and network modelling, in which simplified flow equations are solved in an idealized pore network extracted from the real geometry (Blunt et al. 2013).

Since the first pioneering work (Fatt 1956), pore network models have been widely used to simulate multiphase fluid flow at the pore scale. However, the validity of the pore network models is always limited by the approximations and simplifications used (Ferrari and Lunati 2013). Many pore network models may not be suited for the simulation of multiphase fluid flow in complex porous media (Crawshaw and Boek 2013). One of the most popular approaches is the lattice Boltzmann method (LBM), in which particles move and collide on a discrete lattice in such a way that the average motion of the particles mimics the solution of the Navier–Stokes equations (Shan and Chen 1993; He and Luo 1997). Since the late 1980s, the LBM has emerged as a powerful tool for numerical simulations and investigations of a broad class of complex

flows. The LBM can be considered as a mesoscopic method, occupying the middle ground between the microscopic molecular dynamics and macroscopic fluid dynamics. Unlike pore-network models, which use a simplified representation of the pore geometry and approximate transient flow with a steady-state Poiseuille law, LBM can simulate complex multiphase flows in pore media with natural pore geometries (Bandara et al. 2013). The basic idea of the LBM is to construct simplified kinetic models that incorporate the essential physics of microscopic or mesoscopic processes to ensure that the macroscopic averaged properties obey the desired macroscopic equations (Ghassemi and Pak 2011). LBM has many advantages over the conventional grid-based computational fluid dynamics (CFD) methods, such as volume-of-fluid (VOF) and level-set (LS) methods, especially in handling complex boundaries, flexible reproducing interfaces, incorporating the microscopic interactions between multiple phases, and the parallelisation of the algorithm (Liu et al. 2015a).

Based on the above analysis, at present, the numerical simulation of the CO_2 displacement in porous media is mainly performed using the LBM, and few studies use conventional methods to simulate the displacement process. Gunde et al. (2010) investigated the displacement of oil by CO_2 within the pore structures of a realistic porous geometry ($730 \mu\text{m} \times 450 \mu\text{m}$) derived from processed micro-CT images based on the finite element method. However, the COMSOL simulations require a minimum of 48 h of CPU time to obtain a converged solution for a 10 s displacement process. Berg and Ott (2012) used the phenomenological two-phase extension of Darcy's law to study the stability of CO_2 -brine immiscible displacement in a two/three-dimensional numerical grid. They found that the capillarity, viscosity ratio, gravity and length scales have effects on the stability of the displacement.

Liu et al. (2014) employed LBM to simulate liquid CO_2 (LCO_2) displacing water in a dual-permeability pore network (Fig. 5) and randomly heterogeneous pore network (Fig. 6). The extent and behaviour of the LCO_2 preferential flow (i.e., fingering) is found to depend on the capillary number (Ca). In comparison to the dual-permeability case, in the heterogeneous pore network case, the transition from capillary fingering to viscous fingering occurs at a higher Ca , and the LCO_2 saturation is higher at a low Ca but lower at a high Ca . Yamabe et al. (2015) simulated the supercritical CO_2 -water drainage displacement using LBM in a 3D rock model ($1 \text{ mm} \times 1 \text{ mm} \times 1 \text{ mm}$) that was constructed by a random packing process with a number of spherical grains at a fixed viscosity ratio and at various capillary numbers (by changing the injection pressure, which induces changes in the flow velocity). It was observed that the viscous fingering was dominant at high injection pressures, whereas crossovers of viscous and

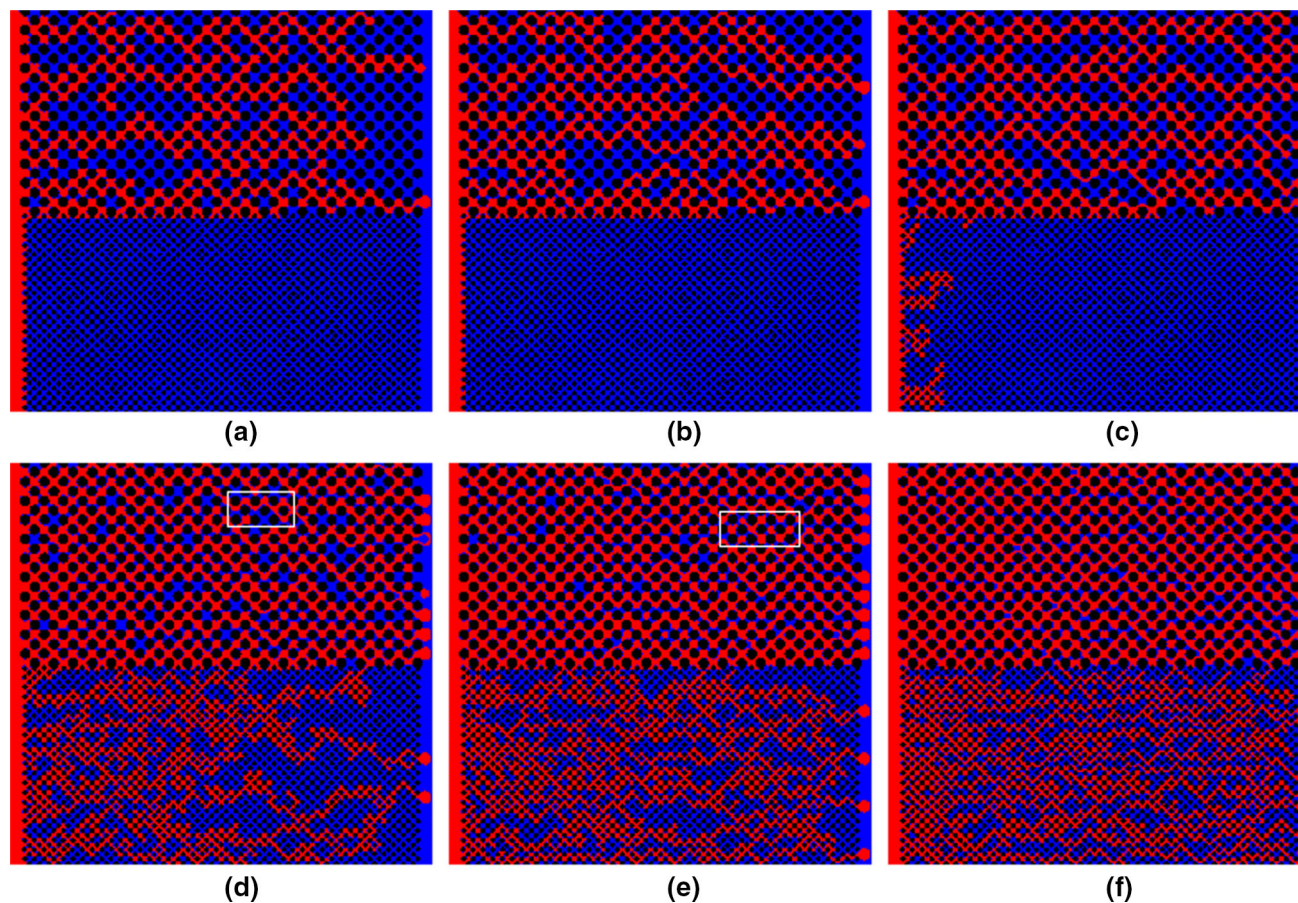


Fig. 5 Final fluid distributions in the dual-permeability microfluidic system at various capillary numbers: **a** $\log Ca = -4.36$, **b** $\log Ca = -4.16$, **c** $\log Ca = -4.06$, **d** $\log Ca = -3.59$, **e** $\log Ca = -3.36$, **f** $\log Ca = -3.06$. LCO₂ and water are shown in red and blue, respectively. (Liu et al. 2014)

capillary fingerings were observed, accompanied by Haines jumps, at low injection pressures. The capillary number and displacement mechanisms are dependent on the geometry of the porous media. Then, they (Yamabe et al. 2016) further evaluated the relationship of V_p -CO₂ saturation, which is the most important relationship in the geophysical monitoring of CCS projects, applying dynamic wave simulation with the FD approach to LB results and the 3D rock model. A lower V_p was observed in the high capillary number case than at a low capillary number at the same saturation. The difference in the V_p response to CO₂ saturation is caused by the CO₂ distribution features. Yang et al. (2015) also used a three-dimensional LBM to simulate the pore-scale scCO₂-oil miscible displacement in upward vertical displacements. At a low kinematic viscosity ratio, a front fingering was found, and a CO₂ breakthrough occurred quickly (Fig. 7a). At a large kinematic viscosity ratio, the displacement was stable with a piston front. The high kinematic viscous oil restrained the buoyancy of the supercritical CO₂ and impeded the displacement with a pore-scale back flow, which might lead to a low oil recovery factor (Fig. 7b). Their study also

indicated that the agravic miscible displacement is slightly quicker than the miscible displacement with gravity in upward miscible displacements.

From the above review, we see that only a limited number of numerical simulation studies have been reported focusing on fundamental processes at the microscopic pore scale during CO₂ injection into a porous formation. These studies also did not systematically investigate the CO₂ displacement mechanisms. During the CO₂ flow in saline aquifers or oil/gas reservoirs, the main physical and chemical interactions among the water, oil/gas and rocks include (Ju et al. 2013): (1) the immiscible and miscible displacement of oil, water and CO₂; (2) convection and diffusion; (3) the phase change and behaviour of *insitu* fluids in flow and mass transfer; (4) precipitation/dissolution and its effects on porosity and permeability; (5) the CO₂ adsorption characteristics in the adsorption of the reservoir. Therefore, in further work, these interactions need to be considered. In addition, although there have been a few studies on the use of LBM for the simulation of the CO₂ displacement process in 3D porous media, the 3D pore structure of real rock has not been used. The main

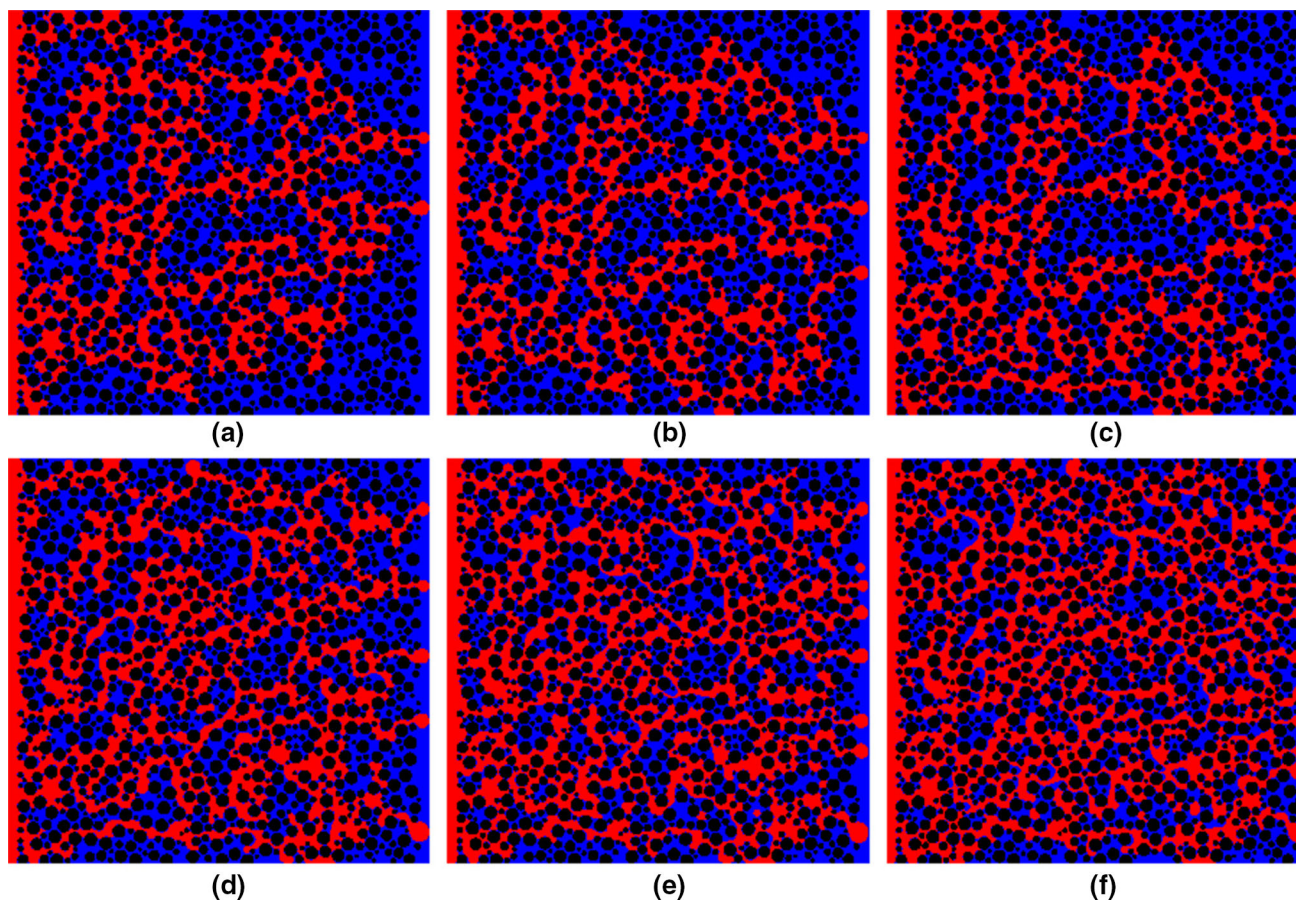


Fig. 6 Final fluid distributions in the randomly heterogeneous system at **a** $\log Ca = -4.36$, **b** $\log Ca = -4.16$, **c** $\log Ca = -4.06$, **d** $\log Ca = -3.59$, **e** $\log Ca = -3.36$, **f** $\log Ca = -3.06$. LCO₂ and water are shown in *red* and *blue*, respectively. (Liu et al. 2014)

reason is that attaining an accurate description of the 3D microstructure of porous rock is difficult, laborious, time-consuming, and economically expensive with the use of advanced 3D CT measurement techniques, e.g., synchrotron X-ray CT (Coker et al. 1996; Spanne et al. 1994), and directly using the 3D microstructure of porous rock for the numerical simulations will entail a massive computational cost. Recently, Ju et al. (2014b) proposed a faster, more accurate, and more efficient reconstruction algorithm (an improved simulated annealing algorithm reconstruction method) to create a 3D model of the porous rock microstructure. On the other hand, the appearance and application of modern high-performance computers offer a new way to study complex flows in a domain with realistic pore geometries.

4 Applications in shale gas

Shale gas, as a renewable energy source, has become more and more important to the worldwide energy supply owing to its low pollution, abundant reserves, and wide

distribution (Curtis 2002; Burnham et al. 2012). It usually has two states stored in shale, that is, free gas in natural cracks and adsorbed gas on the organic matter surfaces (Yin et al. 2016). Generally, a significant part of the shale pores are distributed on the nanometre scale, which results in a large internal surface area (Loucks et al. 2009; Kuila and Prasad, 2013; Mosher et al. 2013). Thus, a large proportion of the shale gas is in an adsorbed state in the nanopores (Chareonsuppanimit et al. 2012). A large number of nanometre pores also lead to the extremely low permeability of the shale (Javadpour et al. 2007; Javadpour 2009; Heller et al. 2014; Hinai et al. 2014). There are many difficulties in shale gas extraction based on the above two issues, and effective methods are urgently required to enhance shale gas recovery (ESGR). Hydraulic fracturing is currently the only fracturing technology utilized in commercial shale gas extraction (Yin et al. 2016). However, water-based fracturing fluids have many drawbacks, including aggravating water scarcity and environmental problems (King 2010; Nagel et al. 2013; Rutqvist et al. 2015). Recently, scCO₂ has attracted widespread attention as a fracturing fluid for use in ESGR (Rogala et al. 2014).

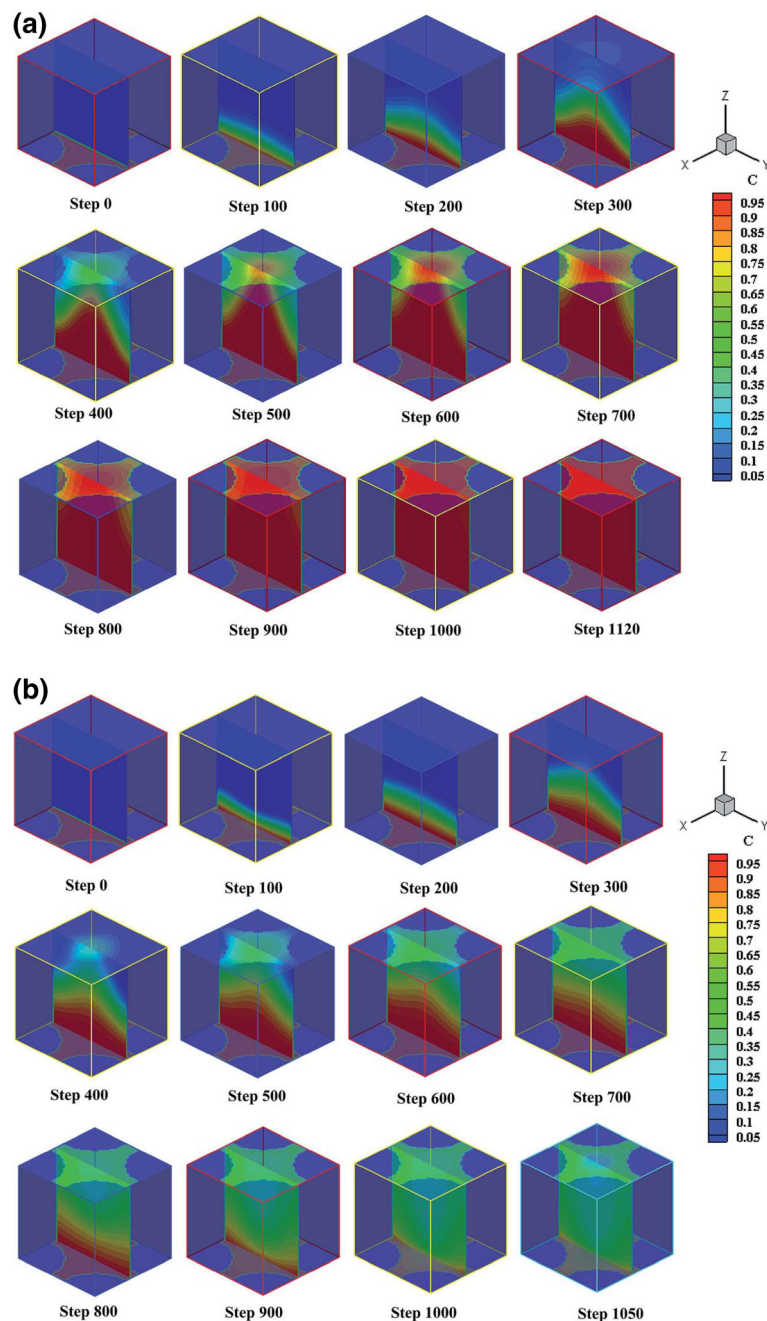


Fig. 7 Simulation results in miscible displacement flows. Kinematic viscosity ratio of CO₂ to oil is **a** 1:1 and **b** 1:15 (Yang et al. 2015)

ScCO₂ has a lower viscosity and similar density to water (Ishida et al. 2012) and its surface tension is almost zero, so in the nanometre pore structure of shale, it could easily flow and induce more complicated fractures. CO₂ injection has also proven to be a potential way to displace shale gas in shale gas formations because the affinity of CO₂ for the shale surface is stronger than that of shale gas (Kang et al. 2011; Heller and Zoback 2014). In addition, shale gas reservoirs are both reservoirs and cap rock, which can realize the effective storage of carbon dioxide. Therefore,

the integration of scCO₂-enhanced shale gas production and geological sequestration is proposed (Fig. 8). When scCO₂ is injected into shale gas reservoirs, four integration effects are generated and three scientific questions need to be solved. A number of studies on the CO₂ fracturing mechanism have been reported (Ishida et al. 2012; Li et al. 2015; Huang et al. 2015; Bennour et al. 2015; Chen et al. 2015), and this paper does not provide a detailed introduction. However, the latter two issues are related to the displacement of multiphase fluid, and there are few studies

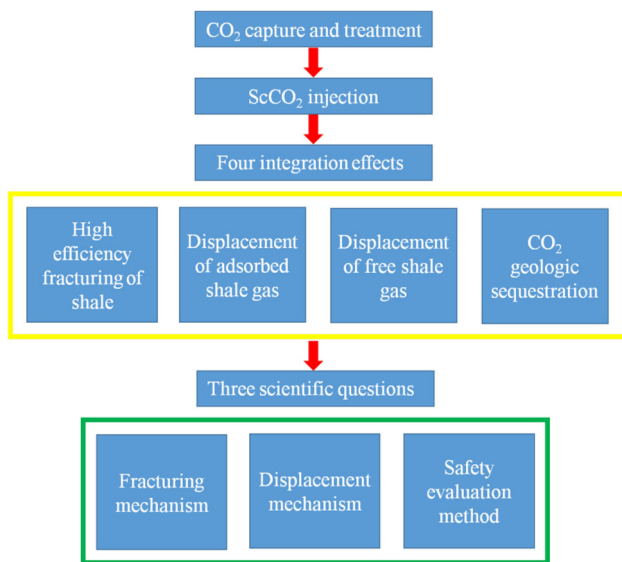


Fig. 8 Integration of scCO₂-enhanced shale gas production and geological sequestration

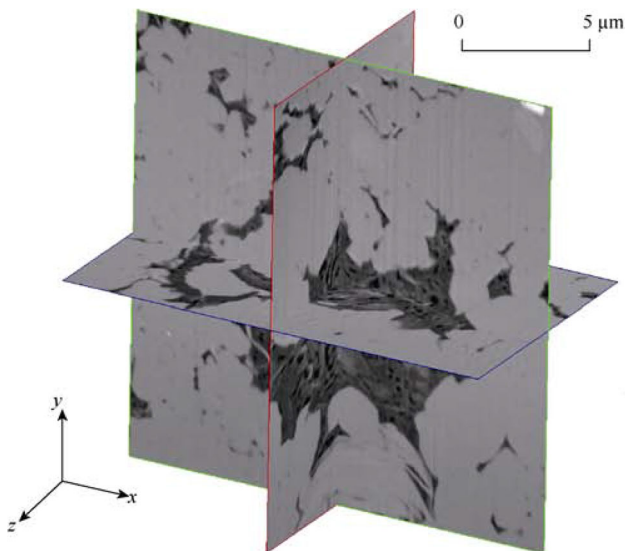


Fig. 9 3D digital core of shale (Sun et al. 2016)

in these areas owing to the special properties of shale gas reservoirs. The existing problems and possible solutions for studying the CO₂ displacement mechanism in the shale pore structure will be introduced in detail below.

4.1 Special properties of shale reservoirs

4.1.1 Nanopore structure

Unlike conventional reservoirs, shale reservoirs are usually dominated by nanometre-scale pores (Nelson 2009; Loucks et al. 2009; Kuila and Prasad 2013; Mosher et al. 2013). According to a previous review on the simulation of CO₂-

formation fluid displacement, at present numerical simulation is the only feasible method to investigate the CO₂ displacement process in nanometre-scale pores, and the quantitative characterization of the shale nanopore structure and pore network modelling are required before the numerical simulation of the CO₂-shale gas displacement can be performed. For this end, several imaging techniques and modelling methods are utilized to characterize the shale pores, such as nano-CT, field emission and scanning electron microscopy (FE-SEM), transmission electron microscopy (TEM), and focused ion beams and scanning electron microscopy (FIB-SEM) (Loucks et al. 2009; Bernard et al. 2012; Chalmers et al. 2012a, b; Curtis et al. 2012; Milliken et al. 2013). Of these methods, the maximum spatial resolution of nano-CT is only 50 nm, and so it cannot satisfy the requirements for shale nanopores of less than 50 nm, which can make the prediction of the fluid migration properties less credible. The spatial resolution of TEM and FE-SEM can satisfy the required standards for nanopore imaging, but they cannot provide 3D pore structures, which is crucial to obtaining the pore shapes and interconnected regions. FIB-SEM can obtain voxel dimensions of 10 nm and is also the only method to characterize the nanopores of the sample by 2D imaging and 3D spatial components, simultaneously. This method is time-consuming and expensive, but many studies have been performed on nanopore characterization using this method because of its accuracy. At present, FIB-SEM has become the mainstream tool for imaging nanopores (Keller et al. 2011; Chalmers et al. 2012a, b; Dewers et al. 2012; Bai et al. 2013). 3D images of shale are first obtained by the FIB-SEM device (Fig. 9) through shape correction, brightness correction, depth-of-field correction and phase distinguishing (Sun et al. 2016), which will make the results of the simulation more accurate and credible.

4.1.2 Knudsen flow

The Knudsen number (Kn) is the ratio of the gas molecular mean free path to the characteristic length. It is an important parameter to define the gas flow regime in shale. The gas transport through shale can be characterized by the value of Kn as continuum flow ($Kn < 0.0001$), slip flow ($0.0001 < Kn < 0.1$), transition flow ($0.1 < Kn < 10$), and free molecular flow ($10 < Kn$) (see Fig. 10) (Javadpour et al. 2007; Sondergeld et al. 2010; Wang et al. 2015). There is a deviation of the gas flow from the continuum hypothesis because of the influence of high Knudsen numbers in shale (Zhang et al. 2014), and other rarefied gas flow mechanisms begin to dominate the gas migration (Wang et al. 2015). Under this condition, Navier–Stokes (N–S) equations with no-slip boundaries will be invalid (Roy et al. 2003). Conventional numerical simulation

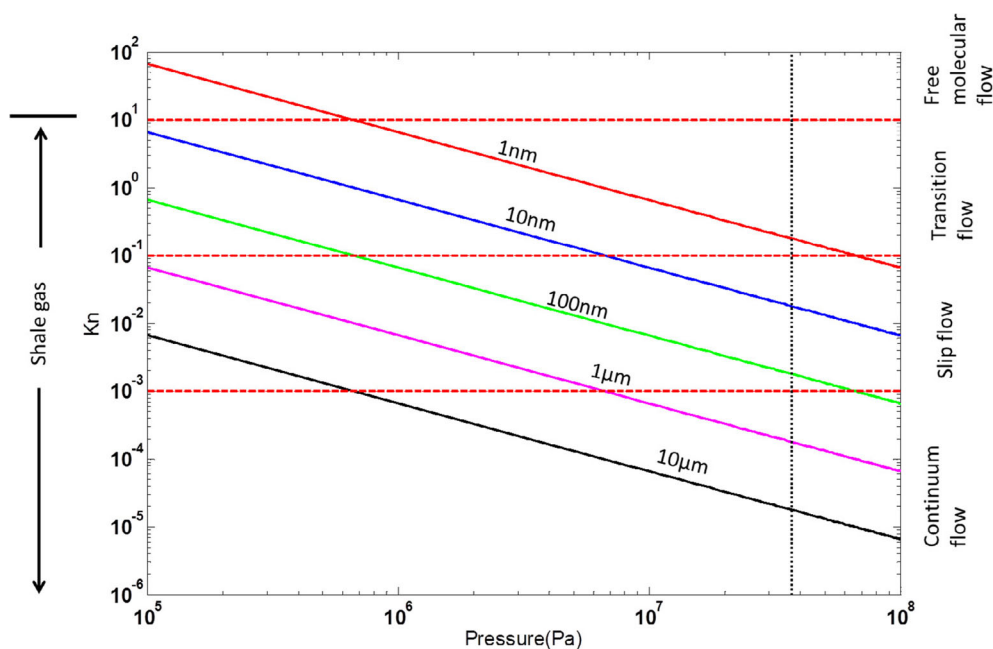


Fig. 10 Relationship among Kn , pore diameter and mean pressure of reservoir at 400 K (Wang et al. 2015)

methods based on the N–S equations also lack the foundation to correctly describe the transport characteristics of shale gas or other rarefied gases.

4.1.3 Adsorption and desorption

Shale contains much organic matter. Previous works suggest that CO₂ has stronger interactions with the organic constituents compared with shale gas because of the appreciable electrostatic moment of the CO₂ molecule (Middleton et al. 2015). Many experimental studies have also revealed that CO₂ can efficiently displace adsorbed shale gas (Kang et al. 2011; Liu et al. 2013a, b; Heller et al. 2014; Luo et al. 2015). However, the displacement mechanisms of adsorbed CH₄ by CO₂ injection are far from being well understood, and quantitatively accurate assessments must be provided. For example, the popular Langmuir model neglects the interaction between CH₄ and CO₂ and does not consider nonidealities in the fluid phases (Middleton et al. 2015). Recently, Shi and Durucan (2003) developed a bidisperse pore-diffusion model for the displacement and desorption of CH₄ in coal by CO₂ injection. Wu et al. (2015) and Yuan et al. (2015) first employed molecular dynamics (MD) simulations to study the displacement of adsorbed CH₄ by CO₂ injection in carbon nanochannels, and they obtained the breakthrough time and front shape of the CO₂. However, to the best of our knowledge, there have been few related reports about the CO₂–CH₄ displacement structures in the slit pore. The adsorption and desorption of gas can induce slit pore changes and it provides feedback that impacts the gas flow.

For example, the primary slit pore of shale narrows because of CO₂ adsorption-induced swelling (see Fig. 11, marked A) (Yin et al. 2016). Therefore, these issues cause great difficulties in the accurate simulation of the CO₂–CH₄ displacement process.

4.2 LB-MD multiscale method

Molecular dynamics (MD) simulation is an effective method to study complex flows at the nanoscale (Li et al. 2010). In MD simulations, the fluid behaviour is described by the motion of the individual particles interacting with each other via intermolecular potentials (Koplik and Banavar 1995). As a result, it is only suitable to simulate fluid behaviours at the nanoscale owing to the limitation of computation cost (Zhao et al. 2016). LBM, as an intermediate method between continuum and atomistic simulations, is considered to have tremendous potential for simulating the fluid flow at the meso-scale, and detailed information on it has been presented in Sect. 2.2. However, the interaction force between the fluid and rock is assumed to be directly proportional to the density of the fluid in conventional LB models, which has no theory to support it and does not represent the real physical phenomena in certain situations (Liu et al. 2015a, b). To combine the advantages of the two described methods, coupling the LBM and MD is proposed to simulate fluid flows. MD describes the atomistic recognition of the fluid flow process near the walls of the porous media, while LBM is responsible for the rest of the simulation process and decreases the computational cost (Marsh et al. 2010).

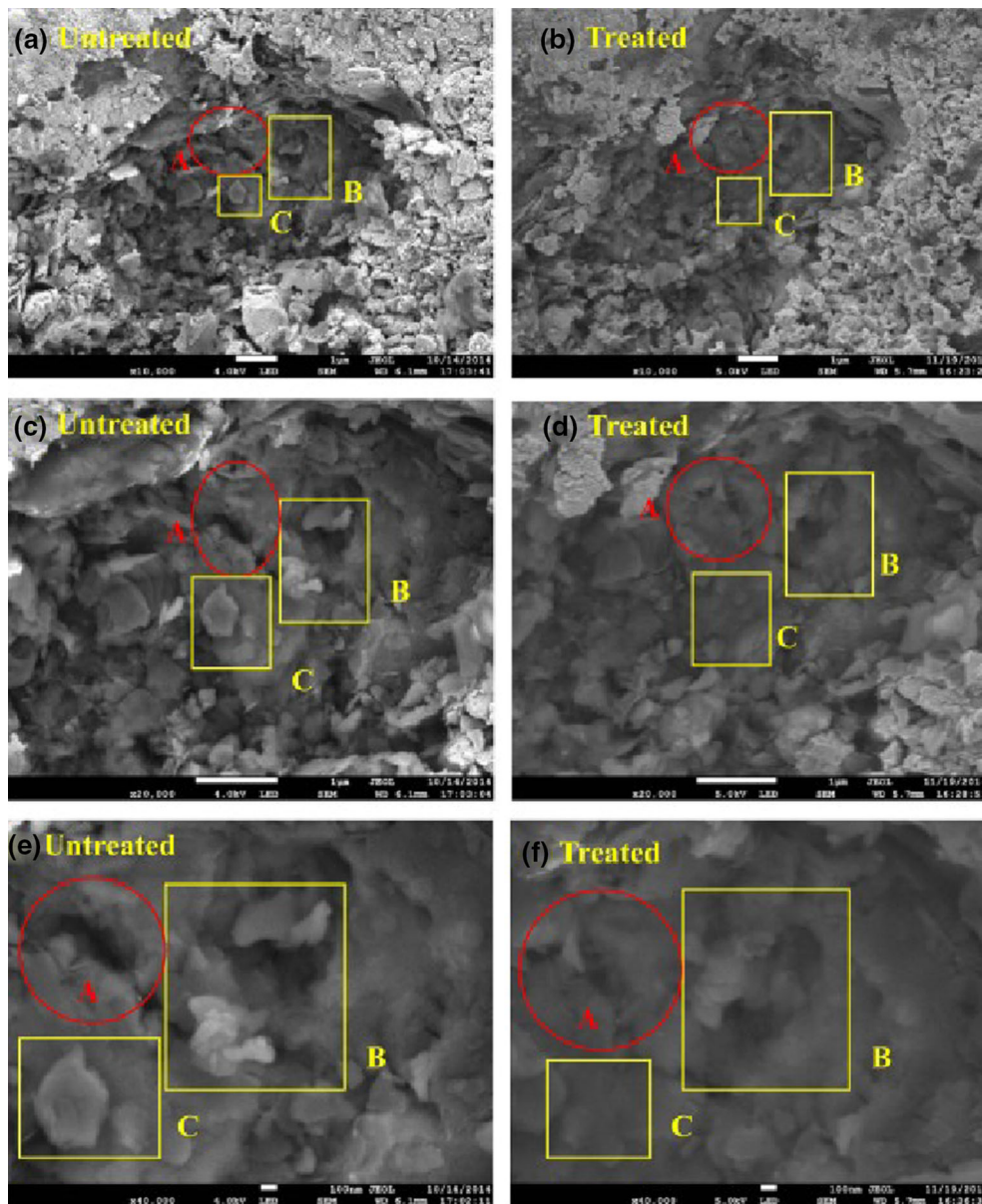


Fig. 11 CO₂ adsorption-induced swelling for shale. **a, c, e** Untreated and **b, d, f** ScCO₂-treated (Yin et al. 2016)

Combinations of the LB and MD methods can be divided into two categories. The first type is the synchronous coupling of the two methods performed by Ahlrichs and Dünweg (1998, 1999) and Fyta et al. (2006). In their studies, the simulation of the motion of DNA, polymers and other macromolecules in water was performed by the method. However, such a synchronous calculation method is very time-consuming for the simulation of fluid flow in porous media owing to the large computation cost of parameter passing between MD and LBM. The second type is the coupling of MD and LB in tandem to settle a problem, rather than simultaneous coupling (Marsh et al. 2010; Choi et al. 2014; Liu et al. 2015a, b; Pereira et al. 2016). MD provides the atomistic recognition of the flow physics

near the walls, while LBM describes the rest of the simulation domain (including the Knudsen flow and absorption/dissolution-induced pore structure changes) and substantially reduces the computational cost.

To accurately simulate the CO₂-shale gas displacement process in the pore structure of shale, the 3D digital core of shale that is obtained by the FIB-SEM device is used directly for the LBM simulation with MD. Considering the computational cost, the coupling of MD and LB in tandem is employed to simulate the CO₂-shale gas displacement process (Fig. 12).

First, the interaction forces between CO₂-CH₄ are obtained from the P-R EOS calculation (Liu et al. 2015a, b), and the shale matrix-CO₂/CH₄ interaction

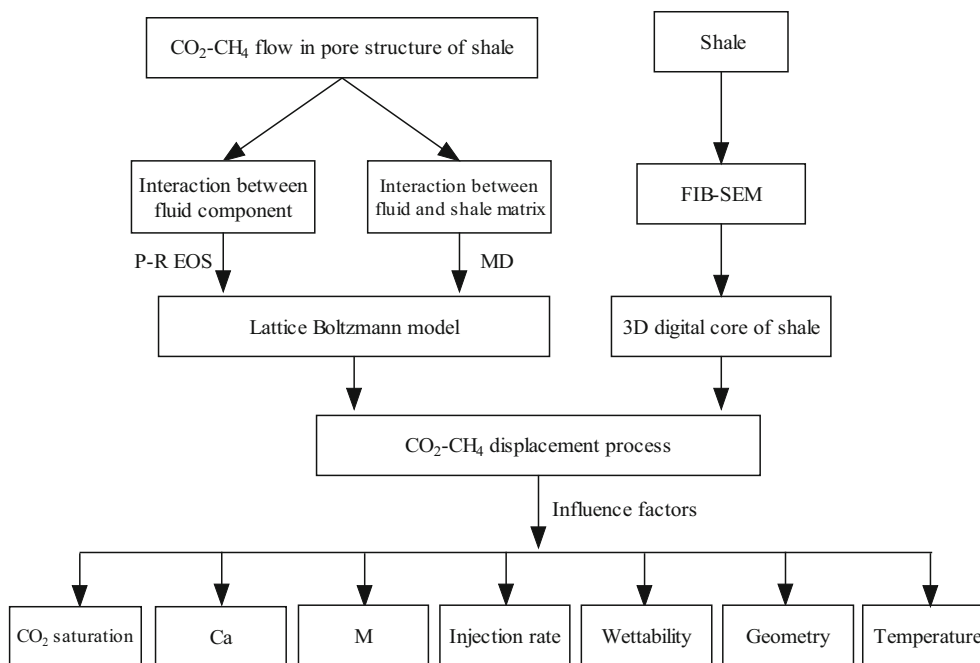


Fig. 12 Schematic diagram of the workflow

(including the displacement of adsorbed CH₄ by CO₂ and the interaction force of fluids-shale) is acquired from the MD simulation. According to the MD simulation, we can calculate the interfacial tension of CO₂/CH₄, the density of CO₂/CH₄ and the concentration of CO₂/CH₄. Then, we run the lattice Boltzmann simulation based on the 3D digital core of shale to obtain the real and whole CO₂-CH₄ displacement process.

5 Conclusions

CO₂-formation fluid displacement at the pore scale is a key issue in CO₂ sequestration and enhanced oil/gas recovery. The current situation and limitations of experiments and numerical simulations in studying the CO₂-formation fluid displacement at the pore scale are described in detail. From the review, we can conclude that there are many influencing factors for CO₂ displacement at the pore scale, e.g., displacement type, effective porosity, flow rate, Ca and M. The use of MRI or X-ray CT and the observation of the fluid displacement in fabricated micromodels are recognized as effective approaches to detect and observe the CO₂-formation fluid displacement processes. The LBM can precisely simulate the CO₂-formation fluid displacement processes in a 2D or 3D complex pore structure, but at the present, realistic rock pore geometries are not used directly to simulate the displacement process based on LBM. Various enhancements to overcome the limitations of experiments and numerical simulations in studying the

CO₂-formation fluid displacement are suggested. Applications of CO₂ displacement have been highlighted for shale gas production. Therefore, the status of research and challenges in the application of CO₂ displacement to enhanced shale gas production are reviewed in the paper. Then, the coupling of MD and LB in tandem is proposed to simulate the CO₂-shale gas displacement process in the 3D images of shale obtained by an FIB-SEM device.

Acknowledgements The authors gratefully acknowledge the financial support of the National Natural Science Foundation of China (Grant Nos. 51374213 and 51674251), the State Key Research Development Program of China (Grant No. 2016YFC0600705), the National Natural Science Fund for Distinguished Young Scholars of China (Grant No. 51125017), the Fund for Innovative Research and Development Group Program of Jiangsu Province (Grant No. 2014-27), the Science Fund for Creative Research Groups of the National Natural Science Foundation of China (Grant No. 51421003), and the Priority Academic Program Development of the Jiangsu Higher Education Institutions (PAPD 2014).

Open Access This article is distributed under the terms of the Creative Commons Attribution 4.0 International License (<http://creativecommons.org/licenses/by/4.0/>), which permits unrestricted use, distribution, and reproduction in any medium, provided you give appropriate credit to the original author(s) and the source, provide a link to the Creative Commons license, and indicate if changes were made.

References

- Ahlich P, Dünweg B (1998) Lattice-Boltzmann simulation of polymer-solvent systems. *Int J Mod Phys C* 9(8):1429–1438

- Ahlrichs P, Dünweg B (1999) Simulation of a single polymer chain in solution by combining lattice Boltzmann and molecular dynamics. *J Chem Phys* 111(17):8225–8239
- Alemu BL, Aker E, Soldal M, Johnsen Ø, Aagaard P (2013) Effect of sub-core scale heterogeneities on acoustic and electrical properties of a reservoir rock: A CO₂ flooding experiment of brine saturated sandstone in a computed tomography scanner. *Geophys Prospect* 61(1):235–250
- Al-Housseiny TT, Tsai PA, Stone HA (2012) Control of interfacial instabilities using flow geometry. *Nat Phys* 8:747–750
- Allen SK, Plattner GK, Nauels A, Xia Y, Stocker TF (2014) Climate change 2013: the physical science basis. An overview of the working group I contribution to the fifth assessment report of the intergovernmental panel on climate change (IPCC). In: EGU General Assembly Conference, vol 16. EGU general assembly conference abstracts
- Bai B, Elgmati M, Zhang H, Wei M (2013) Rock characterization of Fayetteville shale gas plays. *Fuel* 105:645–652
- Bandara UC, Tartakovsky AM, Oostrom M, Palmer BJ, Grate J, Zhang C (2013) Smoothed particle hydrodynamics pore-scale simulations of unstable immiscible flow in porous media. *Adv Water Resour* 62(12):356–369
- Bennour Z, Ishida T, Nagaya Y, Chen Y, Nara Y, Chen Q, Sekine K, Nagana Y (2015) Crack extension in hydraulic fracturing of shale cores using viscous oil, water, and liquid carbon dioxide. *Rock Mech Rock Eng* 48(4):1463–1473
- Berg S, Ott H (2012) Stability of CO₂–brine immiscible displacement. *Int J Greenh Gas Control* 11(6):188–203
- Berg S, Oedai S, Landman AJ, Brussee N, Boele M, Valdez R, Gelder KV (2010) Miscible displacement of oils by carbon disulfide in porous media: experiments and analysis. *Phys Fluids* 22(11):113102–113102-14
- Berg S, Oedai S, Ott H (2013a) Displacement and mass transfer between saturated and unsaturated CO₂–brine systems in sandstone. *Int J Greenh Gas Control* 12(1):478–492
- Berg S, Ott H, Klapp SA, Schwing A, Neiteler R, Brussee N, Makurat A, Leu L, Enzmann F, Schwarz J, Kersten M, Irvine S, Stampanoni M (2013b) Real-time 3D imaging of Haines jumps in porous media flow. *Proc Natl Acad Sci USA* 110(10):3755–3759
- Bernard S, Wirth R, Schreiber A, Schulz HM, Horsfield B (2012) Formation of nanoporous pyrobitumen residues during maturation of the Barnett Shale (Fort Worth Basin). *Int J Coal Geol* 103:3–11
- Birk M, Dapp R, Ruiters NV, Becker J (2014) GPU-based iterative transmission reconstruction in 3D ultrasound computer tomography. *J Parallel Distrib Comput* 74:1730–1743
- Blunt M, Fayers FJ, Orr FM (1993) Carbon dioxide in enhanced oil recovery. *Energy Convers Manag* 34(93):1197–1204
- Blunt MJ, Bijeljic B, Dong H, Gharbi O, Iglauer S, Mostaghimi P, Paluszny A, Pentland C (2013) Pore-scale imaging and modelling. *Adv Water Resour* 51:197–216
- Burnham A, Han J, Clark CE, Wang M, Dunn JB, Palou-Rivera I (2012) Life-cycle greenhouse gas emissions of shale gas, natural gas, coal, and petroleum. *Environ Sci Technol* 46:619–627
- Chalabaud C, Robin M, Lombard JM, Martin F, Egermann P, Bertin H (2009) Interfacial tension measurements and wettability evaluation for geological CO₂ Storage. *Adv Water Resour* 32(1):98–109
- Chalmers GR, Bustin RM, Power IM (2012a) Characterization of gas shale pore systems by porosimetry, pycnometry, surface area, and field emission scanning electron microscopy/transmission electron microscopy image analyses: examples from the Barnett, Woodford, Haynesville, Marcellus, and Doig units. *AAPG Bull* 96:1099–1119
- Chalmers GRL, Ross DJK, Bustin RM (2012b) Geological controls on matrix permeability of Devonian Gas shales in the Horn river and Liard basins, northeastern British Columbia. *Can Int J Coal Geol* 103:120–131
- Chareonsuppanimit P, Mohammad SA, Robinson RL, Gasem KAM (2012) High-pressure adsorption of gases on shales: measurements and modeling. *Int J Coal Geol* 95(2):34–46
- Chen C, Zhang D (2010) Pore-scale simulation of density-driven convection in fractured porous media during geological CO₂ sequestration. *Water Resour Res* 46(11):275–284
- Chen Y, Nagaya Y, Ishida T (2015) Observations of fractures induced by hydraulic fracturing in anisotropic granite. *Rock Mech Rock Eng* 48(6):1–7
- Chiquet P, Daridon JL, Broseta D, Thibeau S (2007) CO₂/water interfacial tensions under pressure and temperature conditions of CO₂ geological storage. *Energy Convers Manag* 48(3):736–744
- Choi SB, Hong MY, Lee JS (2014) Multi-scale approach for the rheological characteristics of emulsions using molecular dynamics and lattice Boltzmann method. *Biomicrofluidics* 8(5):052104
- Cipolla CL, Lolon E, Mayerhofer MJ (2009) Reservoir modeling and production evaluation in shale-gas reservoirs. In: International petroleum technology conference
- Coker DA, Torquato S, Dunsmuir JH (1996) Morphology and physical properties of Fontainebleau sandstone via a tomographic analysis. *J Geophys Res Solid Earth* 101(B8):17497–17506
- Cottin C, Bodiguel H, Colin A (2010) Drainage in two-dimensional porous media: from capillary fingering to viscous flow. *Phys Rev E* 82:689–708
- Crawshaw JP, Boek ES (2013) Multi-scale imaging and simulation of structure, flow and reactive transport for CO₂ storage and EOR in carbonate reservoirs. *Rev Miner Geochem* 77(1):431–458
- Curtis JB (2002) Fractured shale-gas systems. *AAPG Bull* 86:1921–1938
- Curtis ME, Cardott BJ, Sondergeld CH, Rai CS (2012) Development of organic porosity in the Woodford Shale with increasing thermal maturity. *Int J Coal Geol* 103:26–31
- Dehoff KJ, Oostrom M, Zhang C, Grate JW (2012) Evaluation of two-phase relative permeability and capillary pressure relations for unstable displacements in a pore network. *Vadose Zone J* 11(4):2344
- Dewers TA, Heath J, Ewy R, Duranti L (2012) Three-dimensional pore network sand transport properties of a shale gas formation determined from focused ion beam serial imaging. *Int J Oil Gas Coal Technol* 5:229–248
- Edenhofer O, Pichsmaduga R, Sokana Y (2014) Climate change 2014: mitigation of climate change. Contribution of working group III to the fifth assessment report of the intergovernmental panel on climate change. Cambridge University Press, Cambridge, United Kingdom and New York
- Er V, Babadagli T, Xu ZH (2010) Pore-scale investigation of the matrix-fracture interaction during CO₂ injection in naturally fractured oil reservoirs. *Energy Fuels* 24:1421–1430
- Espinoza DN, Santamarina JC (2010) Water-CO₂-mineral systems: interfacial tension, contact angle, and diffusion-implications to CO₂ geological storage. *Water Resour Res* 46(7)
- Fatt I (1956) The network model of porous media. *Pet Trans AIME* 207:144–181
- Ferer M, Ji C, Bromhal GS, Cook J, Ahmadi G, Smith DH (2004) Crossover from capillary fingering to viscous fingering for immiscible unstable flow: experiment and modeling. *Phys Rev E* 70(2):127–150
- Ferrari A (2014) Pore-scale modeling of two-phase ow instabilities in porous media. University of Torino, Turin

- Ferrari A, Lunati I (2013) Direct numerical simulations of interface dynamics to link capillary pressure and total surface energy. *Adv Water Resour* 57:19–31
- Fujii T, Gautier S, Gland N, Boulin P, Norden B, Schmidt-Hattenberger C (2010) Sorption characteristics of CO₂ on rocks and minerals in storing CO₂ processes. *Nat Resour* 1(1):1–10
- Fyta MG, Melchionna S, Kaxiras E, Succi S (2006) Multiscale coupling of molecular dynamics and hydrodynamics: application to DNA translocation through a nanopore. *Multiscale Model Simul* 5(4):1156–1173
- Garcia-Rios M, Luquot L, Soler JM, Cama J (2015) Influence of the flow rate on dissolution and precipitation features during percolation of CO₂-rich sulfate solutions through fractured limestone samples. *Chem Geol* 414:95–108
- Gaus I (2010) Role and impact of CO₂-rock interactions during CO₂ storage in sedimentary rocks. *Int J Greenh Gas Control* 4(1):73–89
- Geiger J, Hunyadfalvi Z, Bogner P (2009) Analysis of small-scale heterogeneity in clastic rocks by using computerized X-ray tomography (CT). *Eng Geol* 103:112–118
- Ghassemi A, Pak A (2011) Pore scale study of permeability and tortuosity for flow through particulate media using lattice boltzmann method. *Int J Numer Anal Meth Geomech* 35(8):886–901
- Gomi T, Koshida K, Miyati T (2007) Development of a nonlinear weighted hybrid cone-beam CT reconstruction for circular trajectories. *Comput Med Imaging Graph* 31:561–569
- Gunde AC, Bera B, Mitra SK (2010) Investigation of water and CO₂ (carbon dioxide) flooding using micro-CT (micro-computed tomography) images of Berea sandstone core using finite element simulations. *Energy* 35(12):5209–5216
- Gunter WD, Gentzis T, Rottenfusser BA, Richardson RJH (1997) Deep coalbed methane in Alberta, Canada: a fuel resource with the potential of zero greenhouse gas emissions. *Energy Convers Manag* 38(96):217–222
- Hajizadeh A, Safekordi A, Farhadpour FA (2011) A multiplepoint statistics algorithm for 3D pore space reconstruction from 2D images. *Adv Water Resour* 34:1256–1267
- He X, Luo LS (1997) Lattice Boltzmann model for the incompressible navier-stokes equation. *J Stat Phys* 88(3–4):927–944
- Heller R, Zoback M (2014) Adsorption of methane and carbon dioxide on gas shale and pure mineral samples. *J Unconv Oil Gas Resour* 8:14–24
- Heller R, Vermeylen J, Zoback M (2014) Experimental investigation of matrix permeability of gas shales. *AAPG Bull* 98(5):975–995
- Hinai AA, Rezaee R, Esteban L, Labani M (2014) Comparisons of pore size distribution: a case from the western Australian gas shale formations. *J Unconv Oil Gas Resour* 8:1–13
- Huang F, Lu YY, Tang JR, Ao X, Jia YZ (2015) Research on erosion of shale impacted by supercritical carbon dioxide jet. *Chin J Rock Mech Eng* 34(4):787–794 (in Chinese)
- Hughes TJ, Honari H, Graham BF, Chauhan AS, Johns ML, May EF (2012) CO₂ sequestration for enhanced gas recovery: new measurements of supercritical CO₂-CH₄ dispersion in porous media and a review of recent research. *Int J Greenh Gas Control* 9:457–468
- Hunt PK, Engler P, Bajsarowicz C (1988) Computed tomography as a core analysis tool: applications, instrument evaluation, and image improvement techniques. *J Pet Technol* 40(9):1203–1210
- IEA (2013) Technology roadmap: carbon capture and storage. <http://www.iea.org/publications/freepublications/publication/technology-roadmap-carboncapture-and-storage-2013.html>
- Ishida T, Aoyagi K, Niwa T, Chen Y, Murata S, Chen Q, Nakayama Y (2012) Acoustic emission monitoring of hydraulic fracturing laboratory experiment with supercritical and liquid CO₂. *Geophys Res Lett* 39:440–453
- Javadpour F (2009) Nanopores and apparent permeability of gas flow in Mudrocks (shales and siltstone). *J Can Pet Technol* 48:16–21
- Javadpour F, Fisher D, Unsworth M (2007) Nano-scale gas flow in shale sediments. *J Can Pet Technol* 46(10):55–61
- Ju B, Wu YS, Qin J (2013) Computer modeling of the displacement behavior of carbon dioxide in undersaturated oil reservoirs. *Oil Gas Sci Technol* 70(6):951–965
- Ju Y, Xie HP, Zheng ZM, Lu JB, Mao LT, Gao F, Peng RD (2014a) Visualization of the complex structure and stress field inside rock by means of 3D printing technology. *Chin Sci Bull* 59(36):5354–5365
- Ju Y, Zheng J, Epstein M, Sudak L, Wang J, Zhao X (2014b) 3d numerical reconstruction of well-connected porous structure of rock using fractal algorithms. *Comput Methods Appl Mech Eng* 279(9):212–226
- Kang SM, Fathi E, Ambrose R, Akkutlu I, Sigal R (2011) Carbon dioxide storage capacity of organic-rich shales. *SPE J* 16:842–855
- Kazemifar F, Blois G, Kyritsis DC, Christensen KT (2016) Quantifying the flow dynamics of supercritical CO₂-water displacement in a 2D porous micromodel using fluorescent microscopy and microscopic PIV. *Adv Water Resour* 95:352–368
- Keller LM, Holzer L, Wepf R, Gasser P, Munch B, Marschall P (2011) On the application of focused ion beam nanotomography in characterizing the 3D pore space geometry of Opalinusclay. *Phys Chem Earth* 36:1539–1544
- King GE (2010) Thirty years of gas shale fracturing: what have we learned. In: *SPE annual technical conference and exhibition, Florence, SPE*, p 133456
- Koide H, Tazaki Y, Noguchi Y, Nakayama S, Iijima M, Ito K, Shindo Y (1992) Subterranean containment and long-term storage of carbon dioxide in unused aquifers and in depleted natural gas reservoirs. *Energy Convers Manag* 33:619–626
- Koplik J, Banavar JR (1995) Continuum deductions from molecular hydrodynamics. *Annu Rev Fluid Mech* 27(1):257–292
- Kuila U, Prasad M (2013) Specific surface area and pore-size distribution in clays and shales. *Geophys Prospect* 61(2):341–362
- Lenormand R, Touboul E, Zarcone C (1988) Numerical models and experiments on immiscible displacements in porous media. *J Fluid Mech* 189(9):165–187
- Li Y, Xu J, Li D (2010) Molecular dynamics simulation of nanoscale liquid flows. *Microfluid Nanofluid* 9:1011–1031
- Li X, Feng Z, Han G, Elsworth D, Marone C, Saffer D (2015) Hydraulic fracturing in shale with H₂O, CO₂ and N₂. In: *US rock mechanics/geomechanics symposium*
- Lindquist WB, Lee SM, Coker DA, Jones KW, Spanne P (1996) Medial axis analysis of void structure in three-dimensional tomographic images of porous media. *J Geophys Res Solid Earth* 101(B4):8297–8310
- Liu Y, Zhao Y, Zhao J, Song Y (2011) Magnetic resonance imaging on CO₂ miscible and immiscible displacement in oil-saturated glass beads pack. *Magn Reson Imaging* 29(8):1110–1118
- Liu FY, Ellett K, Xiao YT, Rupp JA (2013a) Assessing the feasibility of CO₂ storage in the New Albany Shale (Devonian–Mississippian) with potential enhanced gas recovery using reservoir simulation. *Int J Greenh Gas Control* 17:111–126
- Liu X, Zhu YF, Gong B, Yu JP, Cui ST (2013b) From molecular dynamics to lattice Boltzmann: a new approach for pore-scale modeling of multi-phase flow. *Pet Sci* 12(2):282–292
- Liu H, Valocchi AJ, Werth C, Kang Q, Oostrom M (2014) Pore-scale simulation of liquid CO₂ displacement of water using a two-phase lattice Boltzmann model. *Adv Water Resour* 73:144–158
- Liu H, Zhang Y, Valocchi AJ (2015a) Lattice Boltzmann simulation of immiscible fluid displacement in porous media: homogeneous versus heterogeneous pore network. *Phys Fluids* 27(5):052103-1-17

- Liu SY, Zhang Y, Xing WL, Jian WW, Liu ZY, Li TT, Song YC (2015b) Laboratory experiment of CO₂-CH₄ displacement and dispersion in sandpicks in enhanced gas recovery. *J Nat Gas Sci Eng* 26:1585–1594
- Loucks RG, Reed RM, Ruppel SC, Jarvie DM (2009) Morphology, genesis, and distribution of nanometer-scale pores in siliceous mudstones of the Mississippian Barnett Shale. *J Sediment Res* 79:848–865
- Luo XR, Wang SZ, Wang ZG, Jing ZF, Lv M, Zhai ZD, Han T (2015) Adsorption of methane, carbon dioxide and their binary mixtures on Jurassic shale from the Qaidam Basin in China. *Int J Coal Geol* 150:210–223
- Marsh DD, Vanka SP, Marsh DD, Vanka SP (2010) Multiscale MD/LBM simulations of flow in complex nano/micro channels. In: ASME 2010 international mechanical engineering congress and exposition, pp 735–742
- Middleton RS, Carey JW, Currier RP, Hyman JD, Kang QJ, Karra S, Jiménez-Martínez J, Porter ML, Viswanathan HS (2015) Shale gas and non-aqueous fracturing fluids: opportunities and challenges for supercritical CO₂. *Appl Energy* 147(3):500–509
- Milliken KL, Rudnicki M, Awwiller DN, Zhang T (2013) Organic matter-hosted pore system, Marcellus formation (Devonian), Pennsylvania. *AAPG Bull* 97:177–200
- Morais S, Liu N, Diouf A, Bernard D, Lecoutre C, Garrabos Y, Marre S (2016) Monitoring CO₂ invasion processes at the pore scale using geological labs on chip. *Lab Chip* 16:3493–3502
- Mosher K, He J, Liu Y, Rupp E, Wilcox J (2013) Molecular simulation of methane adsorption in micro- and mesoporous carbons with applications to coal and gas shale systems. *Int J Coal Geol* 109–110(2):36–44
- Nagel NB, Sanchez-Nagel MA, Zhang F, Garcia X, Lee B (2013) Coupled numerical evaluations of the geo-mechanical interactions between a hydraulic fracture stimulation and a natural fracture system in shale formations. *Rock Mech Rock Eng* 46:581–609
- Nelson PH (2009) Pore throat sizes in sandstones, tight sandstones, and shales. *AAPG Bull.* 93:1–13
- Nordbotten JM, Celia MA, Bachu S (2005) Injection and storage of CO₂ in deep saline aquifers: analytical solution for CO₂ plume evolution during injection. *Transp Porous Media* 58(3):339–360
- Pereira AO, Lara LS, Miranda CR (2016) Combining molecular dynamics and lattice boltzmann simulations: a hierarchical computational protocol for microfluidics. *Microfluid Nanofluid* 20(2):1–15
- Riazi M, Sohrabi M, Bernstone C, Jamiolahmady M, Ireland S (2011) Visualisation of mechanisms involved in CO₂ injection and storage in hydrocarbon reservoirs and water-bearing aquifers. *Chem Eng Res Des* 89(9):1827–1840
- Rogala A, Ksiezniak K, Krzysiek J, Hupka J (2014) Carbon dioxide sequestration during shale gas recovery. *Physicochem Probl Miner Process* 50(2):681–692
- Roy S, Raju R, Chuang HF, Cruden BA, Meyyappan M (2003) Modeling gas flow through microchannels and nanopores. *J Appl Phys* 93:4870–4879
- Rutqvist J, Rinaldi AP, Cappa F, Moridis GJ (2015) Modeling of fault activation and seismicity by injection directly into a fault zone associated with hydraulic fracturing of shale-gas reservoirs. *J Pet Sci Eng* 127:377–386
- Schlüter S, Sheppard A, Brown K, Wildenschild D (2014) Image processing of multiphase images obtained via X-ray microtomography: a review. *Water Resour Res* 50(4):3615–3639
- Seo JG (2004) Experimental and simulation studies of sequestration of supercritical carbon dioxide in depleted gas reservoirs. Texas A&M University, College Station
- Seo JG, Mamora DD (2005) Experimental and simulation studies of sequestration of supercritical carbon dioxide in depleted gas reservoirs. *J Energy Resour Technol* 127(1):1–6
- Shan X, Chen H (1993) Lattice Boltzmann model for simulating flows with multiple phases and components. *Phys Rev E* 47(3):1815–1819
- Shi JQ, Durucan S (2003) A bidisperse pore diffusion model for methane displacement desorption in coal by CO₂ injection. *Fuel* 82:1219–1229
- Shi J, Xue Z, Durucan S (2009) History matching of CO₂ core flooding CT scan saturation profiles with porosity dependent capillary pressure. *Energy Procedia* 1(1):3205–3211
- Shi J, Xue Z, Durucan S (2011a) Supercritical CO₂ core flooding and imbibition in Berea sandstone -CT imaging and numerical simulation. *Energy Procedia* 4:5001–5008
- Shi J, Xue Z, Durucan S (2011b) Supercritical CO₂ core flooding and imbibition in Tako sandstone-influence of sub-core scale heterogeneity. *Int J Greenh Gas Control* 5(1):75–87
- Sondergeld CH, Newsham KE, Comisky JT, Rice MC, Rai CS (2010) Petrophysical considerations in evaluating and producing shale gas resources. In: SPE unconventional gas conference, Society of Petroleum Engineers
- Song Y, Jiang L, Liu Y, Yang M, Zhao Y, Zhu N, Dou B, Abudula A (2012) An experimental study on CO₂/water displacement in porous media using high-resolution magnetic resonance imaging. *Int J Greenh Gas Control* 10(9):501–509
- Song Y, Yang W, Wang D, Yang M, Jiang L, Liu Y, Zhao YC, Dou BL (2014) Magnetic resonance imaging analysis on the in situ mixing zone of CO₂ miscible displacement flows in porous media. *J Appl Phys* 115(24):244904–244911
- Spanne P, Thovert JF, Jacquín CJ, Lindquist WB, Jones KW, Adler PM (1994) Synchrotron computed microtomography of porous media: topology and transports. *Phys Rev Lett* 73:2001–2004
- Suekane T, Sokawa S, Iwatani S, Tsushima S, Hirai S (2005) Behavior of supercritical CO₂ injected into porous media containing water. *Energy* 30(11):2370–2382
- Suekane T, Ishii T, Tsushima S, Tsushima S, Hirai S (2006) Migration of CO₂ in porous media filled with water. *J Therm Sci Technol* 1(1):1–11
- Suekane T, Furukawa N, Tsushima S, Tsushima S, Hirai S, Kiyota M (2009) Application of MRI in the measurement of two-phase flow of supercritical CO₂ and water in porous rocks. *J Porous Media* 12(2):143–151
- Sun L, Wang XQ, Jin X, Li JM, Wu ST (2016) Three dimensional characterization and quantitative connectivity analysis of micro/nano pore space. *Pet Explor Dev* 43(3):490–498
- Wang Y, Zhang CY, Wei N, Oostrom M, Wietsma TW, Li XC, Bonneville A (2013) Experimental study of crossover from capillary to viscous fingering for supercritical CO₂-water displacement in a homogeneous pore network. *Environ Sci Technol* 47:212–218
- Wang JJ, Chen L, Kang QJ, Rahman SS (2015) The lattice Boltzmann method for isothermal micro-gaseous flow and its application in shale gas flow: a review. *Int J Heat Mass Transf* 95:94–108
- Wellington SL, Vinegar HJ (1985) CT studies of surfactant-induced CO₂ mobility control. In: SPE annual technical conference and exhibition, SPE-14393-MS
- Wellington SL, Vinegar HJ (1987) X-ray computerized tomography. *J Pet Technol* 39(8):885–898
- Wildenschild D, Sheppard AP (2013) X-ray imaging and analysis techniques for quantifying pore-scale structure and processes in subsurface porous medium systems. *Adv Water Resour* 51(1):217–246
- Wu Q (2014) Investigation of fluids flow behavior in nano-scale channels by using optic imaging system. Missouri University of Science and Technology, Rolla
- Wu HA, Chen J, Liu H (2015) Molecular dynamics simulations about adsorption and displacement of methane in carbon nanochannels. *J Phys Chem C* 119(24):13652–13657

- Xiong Q, Baychev TG, Jivkov AP (2016) Review of pore network modelling of porous media: experimental characterisations, network constructions and applications to reactive transport. *J Contam Hydrol* 192:101–117
- Yamabe H, Tsuji T, Liang Y, Matsuoka T (2015) Lattice Boltzmann simulations of supercritical CO₂-water drainage displacement in porous media: CO₂ saturation and displacement mechanism. *Environ Sci Technol* 49(1):537–543
- Yamabe H, Tsuji T, Liang Y, Matsuoka T (2016) Influence of fluid displacement patterns on seismic velocity during supercritical CO₂ injection: simulation study for evaluation of the relationship between seismic velocity and CO₂ saturation. *Int J Greenh Gas Control* 46:197–204
- Yang W, Zhang L, Liu Y, Zhao Y, Jiang L, Yang M, Wang ZG, Wang DY, Song YC (2015) Dynamic stability characteristics of fluid flow in CO₂ miscible displacements in porous media. *RSC Adv* 5(44):34839–34853
- Yin H, Zhou J, Jiang Y, Xian X, Liu Q (2016) Physical and structural changes in shale associated with supercritical CO₂ exposure. *Fuel* 184:289–303
- Yuan Q, Zhu X, Lin K, Zhao YP (2015) Molecular dynamics simulations of the enhanced recovery of confined methane with carbon dioxide. *Phys Chem Chem Phys* 17(47):31887–31893
- Zahid U, Lim Y, Jung J, Han C (2011) CO₂ geological storage: a review on present and future prospects. *Korean J Chem Eng* 28(3):674–685
- Zhang C, Oostrom M, Wietsma TW, Grate JW, Warner MG (2011a) Influence of viscous and capillary forces on immiscible fluid displacement: pore-scale experimental study in a water-wet micromodel demonstrating viscous and capillary fingering. *Energy Fuels* 25(8):3493–3505
- Zhang CY, Oostrom M, Grate JW, Wietsma TW, Warner MG (2011b) Liquid CO₂ displacement of water in a dual-permeability pore network micromodel. *Environ Sci Technol* 45:7581–7588
- Zhang R, Ai T, Li HG, Zhang ZT, Liu JF (2013) 3D reconstruction method and connectivity rules of fracture networks generated under different mining layouts. *Int J Min Sci Technol* 23(6):863–871
- Zhang X, Xiao L, Shan X, Guo L (2014) Lattice boltzmann simulation of shale gas transport in organic nano-pores. *Sci Rep* 4(6183):536–538
- Zhao Y, Song Y, Liu Y, Jiang L, Zhu N (2011a) Visualization of CO₂ and oil immiscible and miscible flow processes in porous media using NMR micro-imaging. *Pet Sci* 8(2):183–193
- Zhao Y, Song Y, Liu Y, Liang H, Dou B (2011b) Visualization and measurement of CO₂ flooding in porous media using MRI. *Ind Eng Chem Res* 50(8):4707–4715
- Zhao J, Yao J, Zhang L, Sui H, Zhang M (2016) Pore-scale simulation of shale gas production considering the adsorption effect. *Int J Heat Mass Transf* 103:1098–1107